Science Applications of Phased Array Radars

BAMS Article

Science Applications of Phased Array Radars

Pavlos Kollias, Robert Palmer, David Bodine, Toru Adachi, Howie Bluestein, John Y. N. Cho, Casey Griffin, Jana Houser, Pierre. E. Kirstetter, Matthew R. Kumjian, James M. Kurdzo, Wen Chau Lee, Edward P. Luke, Steve Nesbitt, Mariko Oue, Alan Shapiro, Angela Rowe, Jorge Salazar, Robin Tanamachi, Kristofer S. Tuftedal, Xuguang Wang, Dusan Zrnić, and Bernat Puigdomènech Treserras

ABSTRACT: Phased array radars (PARs) are a promising observing technology, at the cusp of being available to the broader meteorological community. PARs offer near-instantaneous sampling of the atmosphere with flexible beam forming, multifunctionality, and low operational and maintenance costs and without mechanical inertia limitations. These PAR features are transformative compared to those offered by our current reflector-based meteorological radars. The integration of PARs into meteorological research has the potential to revolutionize the way we observe the atmosphere. The rate of adoption of PARs in research will depend on many factors, including (i) the need to continue educating the scientific community on the full technical capabilities and trade-offs of PARs through an engaging dialogue with the science and engineering communities and (ii) the need to communicate the breadth of scientific bottlenecks that PARs can overcome in atmospheric measurements and the new research avenues that are now possible using PARs in concert with other measurement systems. The former is the subject of a companion article that focuses on PAR technology while the latter is the objective here.

KEYWORDS: Atmosphere; Convective-scale processes; Instrumentation/sensors; Radars/ Radar observations

https://doi.org/10.1175/BAMS-D-21-0173.1
Corresponding author: Pavlos Kollias, pavlos.kollias@stonybrook.edu
In final form 29 April 2022

AFFILIATIONS: Kollias—Stony Brook University, State University of New York, Stony Brook, and Brookhaven National Laboratory, Upton, New York; **Palmer and Kirstetter**—Advanced Radar Research Center, and School of Meteorology, University of Oklahoma, Norman, Oklahoma; **Bodine**—Advanced Radar Research Center, University of Oklahoma, Norman, Oklahoma; **Adachi**—Meteorological Research Institute, Japan Meteorological Agency, Tsukuba, Japan; **Bluestein, Shapiro, and Wang**—School of Meteorology, University of Oklahoma, Norman, Oklahoma; **Cho and Kurdzo**—Lincoln Laboratory, Massachusetts Institute of Technology, Lexington, Massachusetts; **Griffin**—State University of New York at Brockport, Brockport, New York; **Houser**—Ohio University, Athens, Ohio; **Kumjian**—The Pennsylvania State University, State College, Pennsylvania; **Lee**—Earth Observing Laboratory, National Center for Atmospheric Research, Boulder, Colorado; **Luke**—Brookhaven National Laboratory, Upton, New York; **Nesbitt**—University of Illinois Urbana–Champaign, Urbana, Illinois; **Oue and Tuftedal**—Stony Brook University, State University of New York, Stony Brook, New York; **Rowe**—University of Wisconsin–Madison, Madison, Wisconsin; **Salazar**—Advanced Radar Research Center, and School of Electrical and Computer Engineering, University of Oklahoma, Norman, Oklahoma; **Tanamachi**—Purdue University, West Lafayette, Indiana; **Zrnić**—NOAA/National Severe Storms Laboratory, and Advanced Radar Research Center, University of Oklahoma, Norman, Oklahoma; **Puigdomènech Treserras**—McGill University, Montreal, Quebec, Canada

For over 60 years, radars have been a key enabler of scientific discoveries in atmospheric research and have become irreplaceable to weather prediction. The same radar returns from natural targets such as clear air turbulence and hydrometeors that were considered to be interference by the military during World War II were treasured by the meteorological community. Since then, a large body of theoretical and experimental work has been accomplished and the measurable properties of radar signals—amplitude, phase, polarization, and frequency—are interpreted in terms of the sizes, shapes, motions, and thermodynamic phase of precipitation particles (e.g., Doviak and Zrnić 2006; Bringi and Chandrasekar 2001; Fabry 2015). Significant advancements in radar technology and digital signal processing have led to the development of sophisticated atmospheric radar systems (Kollias et al. 2020a). Dual-polarization has become indispensable for microphysical studies, quantitative estimation of precipitation amounts (Ryzhkov and Zrnić 2019; Oue et al. 2021; Bukovcic et al. 2020; Zhang et al. 2020; Matrosov et al. 2020), and for data quality control (Zrnić and Ryzhkov 1999; Bachmann and Zrnić 2007; Melnikov et al. 2008). Finally, the Doppler capability has provided a wealth of knowledge in storm dynamics (Protat and Zawadzki 1999, Bousquet et al. 2007; Potvin et al. 2012; North et al. 2017).

Reflector antenna-based radars typically employ the plan position indicator (PPI) scan which maps the radar observables onto polar coordinates with constant elevation angle. If the antenna controlled by the scanner performs a full rotation (360° azimuth swath), the scan is called a surveillance scan; otherwise, it is called a sector scan. In surveillance mode, the low-tilt PPI scan provides the distribution of precipitation in plan view (Fig. 1a). A time sequence of PPIs can be used to capture the evolution and motion of precipitation areas. One full surveillance scan is typically completed within 15–20s. Using a set of PPI scans at different elevations, the precipitation vertical structure can be extracted along a specific azimuth angle approximately every 4–6 min (Fig. 1b). The vertical resolution is often coarse due to the limited number of elevations used in the radar surveillance scan. In addition, two coverage gaps are noticeable: 1) the low-level coverage gap introduced by the Earth's curvature and 2) the "cone-of-silence" at upper levels near the radar location introduced by the maximum elevation used by the radar surveillance scan.

A dense radar network is the only way to address the low-level radar coverage gap (McLaughlin et al. 2009). The poor vertical resolution and the cone-of-silence can be addressed using range–height indicator (RHI) scans, where the antenna scans in elevation at a fixed azimuth (Kollias et al. 2020a). Performing a hybrid PPI–RHI sector scan with a large reflector antenna will result to considerable loss of sampling time due to the acceleration and deceleration of the pedestal (15%–30% depending on the sector size) and adds stresses on the pedestal hardware. This type of hybrid scan is usually employed by reflector antenna-based research radars. The mechanical inertia introduced by using a large reflector antenna placed on a positioner is one aspect of meteorological radars that has remained essentially the same over the past 60 years. This single factor exerts considerable influence on a radar's spatiotemporal sampling, the interpretation of the signals, and quality control of radar observations, and has considerable operations and maintenance implications on operational and research radar networks across the world. In addition, a large reflector antenna offers no flexibility on how to control the radiation pattern (i.e., number of beams and shape of beams).

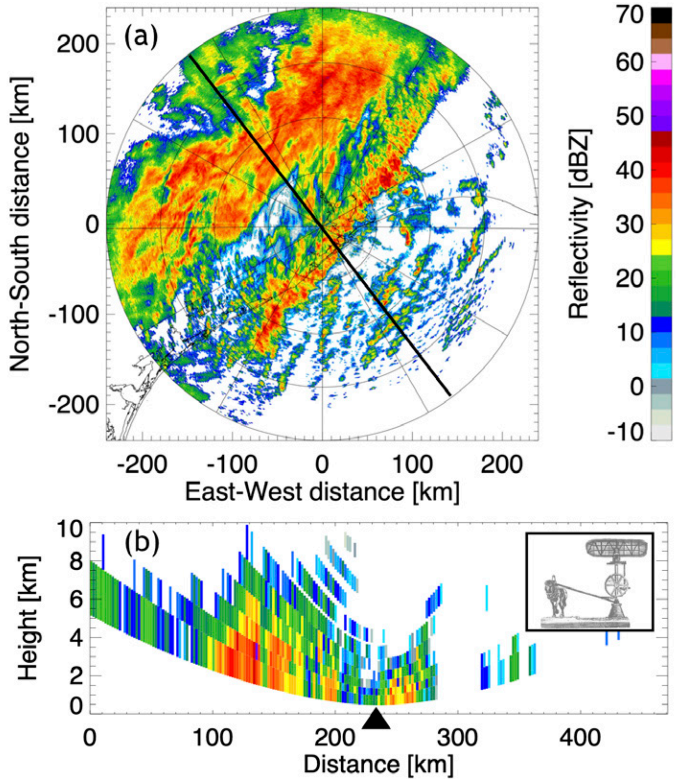

Fig. 1. (a) 0.48° elevation PPI from KHGX, the WSR-88D in the Houston/Galveston, TX, area collected at 0812:07 UTC on 23 Jan 2019 and (b) the reconstructed vertical view of the precipitation along the azimuth line shown on the PPI panel. The triangle indicates the KHGX location. Inset box: analogy of mechanically scanned antennas.

Today, phased array radars (PARs)—designed several decades ago for tracking man-made targets—are a mature, established technology at the cusp of being available to the broader meteorological community (Palmer et al. 2022). Such radars can track or search for targets without moving their antenna. To steer the beam, they rely on wave interactions among signals from a multitude of small antenna elements (Brookner 1985). PARs offer near instantaneous sampling of the atmosphere when and where it is needed without mechanical inertia limitations (Weadon et al. 2009; Heinselman and Torres 2011). In addition, PARs offer the ability to change the shape of the radar beam using imaging from pulse to pulse. Thus, for the first time, researchers take full control of the antenna, the component that connects the radar transceiver with the atmosphere. This offers transformative capabilities for sampling rapidly evolving atmospheric phenomena, utilize advanced clutter and interference mitigation techniques. The all-digital PAR technology (Palmer et al. 2022), the radar can become "software defined," allowing future observational modes to be implemented via software updates rather than expensive and time-consuming hardware changes. Finally, PARs also have higher reliability because they require no moving parts and have graceful degradation of performance.

Despite these advantages, the adoption of PAR technology in atmospheric science will be different in many ways from the early usage of radars in meteorology. Sixty years since the inception of radar use in meteorology, the research community has considerable knowledge and performance expectations. The interpretation of radar returns from atmospheric phenomena is often more challenging than the interpretation of those from man-made targets and depends on well-established high standards on the quality of the amplitude, phase, and polarization measurements. The ongoing debate encompassing the next generation of operational weather radar systems in the United States (Weber et al. 2021) provides an example of our "educated inertia." The companion paper by Palmer et al. (2022) discusses the significant progress on PAR technology and outlines a few outstanding challenges, such as calibration due to the varying beam and polarization characteristics and cost. In this article, a different narrative is introduced where the potential of PARs to revolutionize the way we observed the atmosphere is discussed in a broader sense (beyond the scope of replacing existing operational weather radar networks), anticipating that short-term technological advancements will address current shortcomings in PAR technology and the measurement standards requirements for the scientific applications discussed here are not necessarily those introduced by the National Weather Service (NWS). Our hope is that a concise discussion on the breadth of scientific deadlocks that PARs can overcome in atmospheric measurements and the new research avenues that are now possible using PARs in concert with other measurement systems will increase the number of early PAR adopters and provide federal agencies with the justification to support PAR-based facilities.

Gaps in our scientific knowledge

The need for PAR technology is well documented in past National Research Council reports (e.g., National Research Council 2002), the National Science Foundation (NSF) Radar Workshop in 2012 (Bluestein et al. 2014), and the In Situ and Remote Sensing Capabilities in Convective and Turbulent Environments (C-RITE; Geerts et al. 2018) Community Workshop in 2017. Most recently, the 2021 virtual PAR workshop (Bodine et al. 2021) included a focus on the accessibility of this technology expanding into educational applications and a greater breadth of science applications.

Convective dynamics and severe weather hazards. Since dynamical and microphysical processes in severe convective weather are highly variable in space and time, high-resolution four-dimensional (4D) PAR measurements of wind and polarimetric variables offer tremendous opportunities to elucidate the physical processes underpinning many such phenomena including landfalling tropical cyclones, hailstorms, thunderstorms, tornadoes, and heavy snowfall. Current sampling capabilities of conventional scanning radars often provide insufficient spatial and temporal sampling (Δt) of atmospheric parameters relative to their evolution across finer space and time scales (Fig. 2). Observations using the conventional mechanical scanning strategies, which generally take on the order of 5 min, are deficient, particularly in their ability to scan volumes large enough to entirely cover storms and other atmospheric phenomena of interest (and their near environments) with polarimetric capabilities, a fine beamwidth, and with acceptable data quality (Fig. 2). This is particularly true in colder climates where sensitivity and data quality are prioritized, and PAR's adaptive sampling strategies can address these needs while improving the temporal sampling.

For example, tornadoes require extremely rapid update times to document tornadogenesis and evolutions on the order of 1–10 s (e.g., Bluestein et al. 2010). The use of mobile X-band hybrid phased array and scanning military Doppler radar (MWR-05XP, Bluestein et al. 2010) improved single/dual-Doppler wind retrievals (e.g., French et al. 2013; Bluestein et al. 2016; Liou et al. 2018). Numerous studies of tornadoes using rapid-scan radars have increased our knowledge of tornadogenesis, tornado decay, and tornado debris behavior (Pazmany et al. 2013; French et al. 2014; Wurman and Kosiba 2013; Tanamachi and Heinselman 2016;

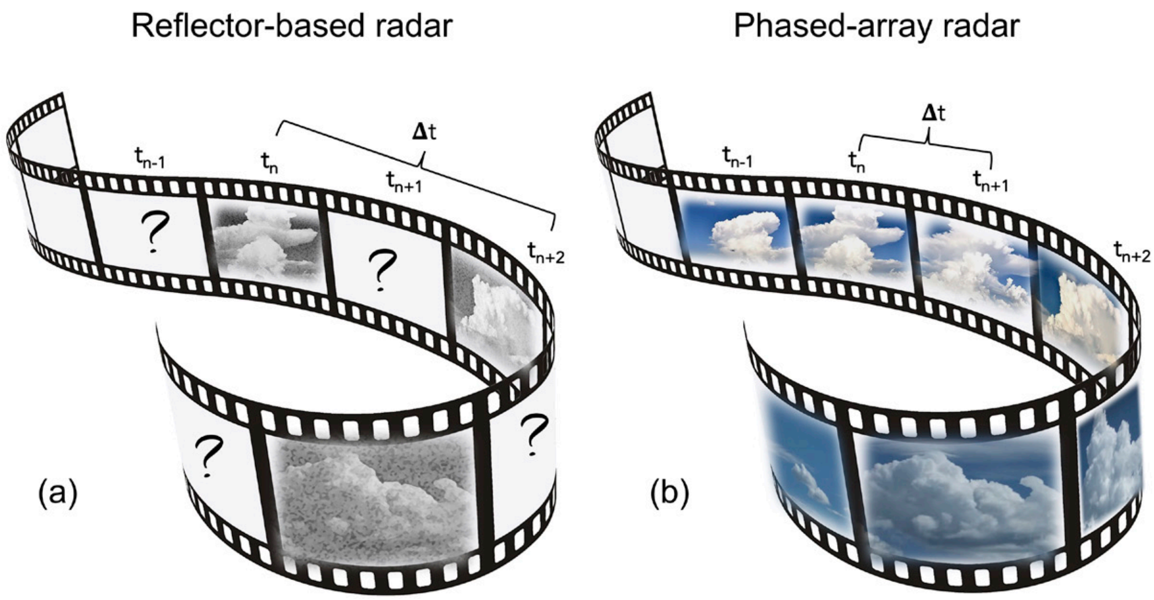

Fig. 2. By analogy to the movie film, (a) reflector-based radars can only capture coarse spatiotemporal resolution information on the cloud life cycle, while (b) phased array radars can offer the sequence of the convective clouds' life cycle at a higher rate (frames per second) and higher spatial (pixel) resolution.

Bluestein et al. 2015, 2019a; Houser et al. 2015, 2016, 2020; Wakimoto et al. 2015, 2016, 2018, 2020; Kurdzo et al. 2017; Wienhoff et al. 2018, 2020; McKeown et al. 2020; Snyder et al. 2020; Wurman et al. 2021), and the relationship between satellite-observed cloud tops and the internal behavior of tornadic supercells (Bluestein et al. 2019b). In addition, studies with PARs revealed the existence of secondary vortices, which evolve on time scales of just a few seconds (Bluestein et al. 2018), and shallow supercells and tornadoes associated with tropical cyclones (Adachi and Mashiko 2020; Morotomi et al. 2020).

While these studies increase our knowledge, many studies also point to the benefits that can be accrued with further rapid-scan polarimetric capabilities. For example, shallow supercells in the outer rainbands of landfalling tropical cyclones (TCs) are considerable generators of significant tornadoes [greater than or equal to Enhanced Fujita (EF)-2 scale; Potter 2007] in the southeastern coastal states of the CONUS (Schultz and Cecil 2009). TC-associated high storm-relative helicity (SRH) and CAPE confined at low levels are favorable for rapidly evolving shallow supercells and tornadoes (Schneider and Sharp 2007). However, specific physical mechanisms of TC tornadoes are still an open question because of difficulties in observing systems having such small spatiotemporal scales (Fig. 3). Adachi and Mashiko (2020) used PAR observations to shed light on this issue, suggesting that PAR is a promising tool for this purpose.

Process rates in convective and stratiform precipitation. Not only have weather radars been crucial to advancing scientific understanding of severe convective storms but they have been key to advancing cloud and precipitation science by improving our understanding of microphysics and their parameterizations in numerical weather prediction (NWP) models. Precipitation is a flux of hydrometeors; polarimetric radar measurements can characterize these hydrometeors. Especially when coupled with detailed microphysical models, one may infer the operation of microphysical processes such as aggregation, riming, and evaporation from spatial polarimetric features called "microphysical fingerprints" (e.g., Kumjian and Ryzhkov 2010, 2012; Andrić et al. 2013; Kumjian and Prat 2014; Kumjian et al. 2012, 2020; Schrom et al. 2015; Oue et al. 2015a,b; 2018; Kalesse et al. 2016; Tobin and Kumjian 2017; Laurencin et al. 2020; Wu et al. 2018, 2021; Tuftedal et al. 2021).

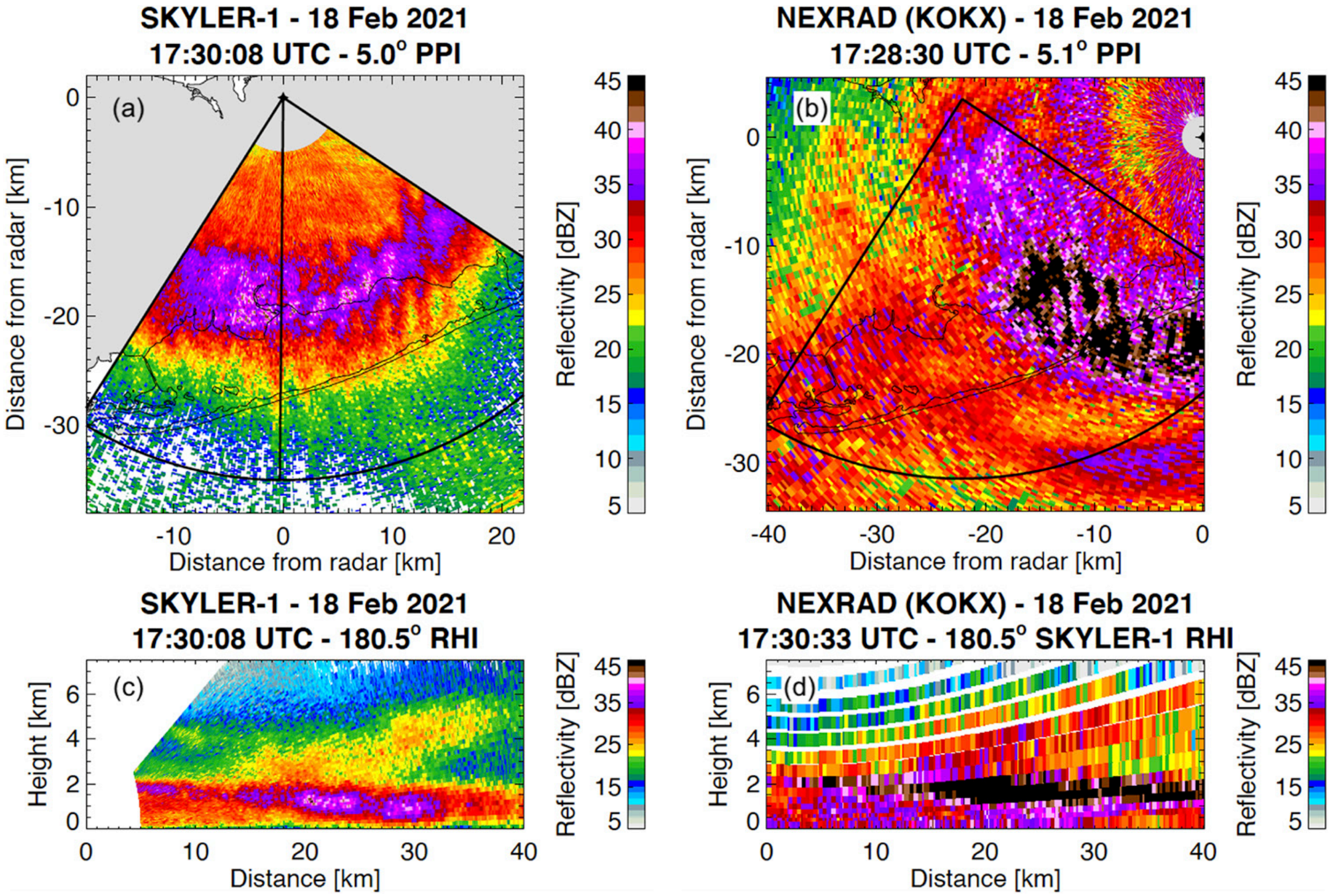

Fig. 3. **(a) Example PPI at 5° from a winter storm on 18 Feb 2021 at 1730:08 UTC in Long Island, NY, from the Raytheon SKYLER-1 system (Kollias et al. 2022) at Stony Brook University; (b) the corresponding PPI from the KOKX WSR-88D at Upton, NY; (c) an SKYLER-1 RHI at azimuth 180.5° collected instantaneously with the PPI; and (d) the corresponding reconstructed vertical structure as captured by all the KOKX PPIs along the SKYLER-1 RHI two-dimensional plane.**

Time resolution is key to monitoring precipitation evolution in rapidly evolving convective processes (e.g., hail growth), mass fluxes (e.g., rain shafts), and related hydrologic hazards. Yet, current reflector antenna-based radar scanning strategies provide only discontinuous sampling due to trading off temporal resolution and data quality for spatial continuity. A common approach is to reconstruct vertical profiles via azimuthal averaging of PPI scans (Ryzhkov et al. 2016). Although useful for bulk assessments of microphysical processes in widespread precipitation (e.g., Kumjian and Lombardo 2017; Tobin and Kumjian 2017; Griffin et al. 2018; Kumjian et al. 2020), this approach is not useful for studying spatially heterogeneous convection (Fig. 3). Further, current dish-type radar scanning strategies do not allow for rapid updates or Lagrangian precipitation shaft tracking, leaving researchers only with "snapshots" of an evolving precipitation system. Phased-array radar complement polarimetry with the temporal dimension required to characterize precipitation fluxes (e.g., time derivatives of polarimetric observations) and would allow such sampling, potentially providing unprecedented information about ongoing precipitation processes.

Quasi-continuous sampling of the precipitation column from low altitudes to cloud top will fill current gaps arising from discontinuous sampling, to better observe warm- and mixed-phase microphysical processes and their interactions that distribute hydrometeor fluxes and shape the vertical structure of precipitation (Kirstetter et al. 2010, 2013; Ryzhkov et al. 2016). An increased vertical resolution of the polarimetric observations is critical to accurately capturing features such as vertical gradients (e.g., Porcacchia et al. 2019) that can be better interpreted with microphysical models to quantify hydrometeor size growth rates (Morrison et al. 2020). When coupled with detailed microphysical models, preliminary studies are indicating such information can be used to retrieve quantitative process rate information (e.g., Schrom et al. 2021).

Convective updrafts. Convective storms transport water vapor and condensate from Earth's surface to the upper troposphere. Convection characteristics including updraft properties such as core size, depth, and updraft magnitude and their evolution throughout the convective cloud lifetime are closely related to environmental factors (e.g., Varble 2018; Grabowski and Morrison 2021; Peters et al. 2021). Because cumulus clouds evolve rapidly, their microphysical and kinematic properties and life cycles are challenging to resolve using conventional observational platforms (e.g., Fridlind et al. 2019; Oue et al. 2019).

The collection of comprehensive observations of convective updrafts using surface-based radars remains challenging. Profiling radar techniques (e.g., Williams 2012; Kumar et al. 2015; Wang et al. 2020) offer limited sampling of individual storms and lack information on the temporal evolution of the convective dynamics. Although multi-Doppler wind retrievals have been used successfully to study kinematic properties of convective updrafts (Lhermitte and Miller 1970; Junyent et al. 2010; North et al. 2017), these analyses are prone to significant errors in the retrieval of the vertical air motion, especially in the upper part of convective storms (Oue et al. 2019). These errors stem from the selected radar volume coverage pattern (VCP), the sampling time for the VCP, the number of radars used, and the added value of advection correction. Using end-to-end simulations Oue et al. (2020) determined that the VCP elevation strategy and sampling time have a significant effect on the retrieved updraft properties above 6 km altitude. In addition, decreasing the VCPs sampling time to less than 2 min improves the impact of the advection correction and thus significantly improves the retrievals.

The Oue et al. (2019) study suggests that the use of rapid-scan radars can substantially improve the quality of convective updrafts retrievals if conducted in a limited spatial domain (Fig. 4). PARs are suitable for limited domain scans (in azimuth and elevation) since they have no time overhead that would be associated with the acceleration and deceleration of a dish antenna at the edges of the sector scan. Profiles of radar observations will document convective dynamics and microphysics from top to bottom, and 3D coverage over the storm life cycle will detail the evolution of the breadth, depth, strength, and tilt of convective updrafts/downdrafts. These crucial measurements will improve our theoretical understanding and monitoring of storms and related hazards, aerosol–convection–precipitation interactions (e.g., Igel and van den Heever 2021), and the next generation of atmospheric models for severe weather prediction.

Clear air studies. Clear air observations in the planetary boundary layer (PBL) rely on passive wind tracers such as low-airspeed insects, chaff, or refractive index irregularities (Bragg scattering). Winds in prestorm environments contain kinematic features (divergence, fronts) that influence storm formation (Doviak and Zrnić 2006; Heinselman et al. 2009; Markowski and Richardson 2011). This information has predictive value to both forecasters and numerical models. Winds between storms are also important as they influence cell evolution and entrainment; their tracers may be Bragg scatterers or nonprecipitating clouds. In addition, a very important feature of clear air returns is the potential for retrieving the average humidity within the PBL (Gossard et al. 1982). Upscale generation of turbulence in the PBL is another phenomenon suitable for research with a PAR. Analysis of the third-order velocity structure function has demonstrated downscale and upscale turbulent energy flux, the former for 3D small-scale turbulence to dissipation, whereas scales larger than 10 km the observed

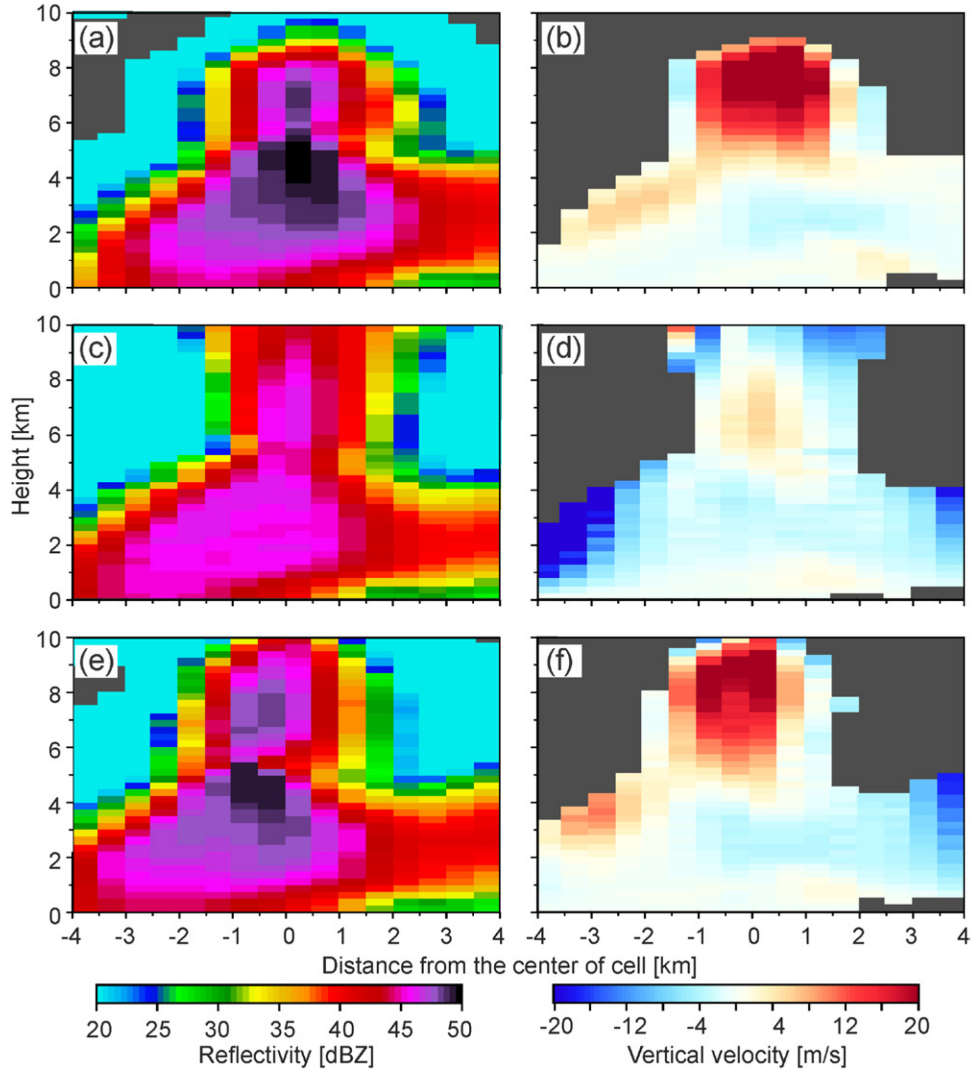

Fig. 4. Vertical cross sections of (a),(c),(e) radar reflectivity and (b),(d),(f) vertical velocity from (a),(b) a cloud model simulation of deep convection; (c),(d) a triple-Doppler wind retrieval using 5-min WSR-88D VCPs; and (e),(f) a triple-Doppler wind retrieval using 3-min VCPs with 60° elevation scans.

transfer was upscale to 2D turbulence (Cho et al. 2001). It has been observed in a hurricane boundary layer (Byrne and Zhang 2013) that "the large-scale parent vortex may gain energy directly from small scales in tropical cyclones." By analogy we submit that a similar gain in energy may occur in some mesoscale convective systems.

A PAR could make the clear air measurements through adaptive scans in space (scanning limited to relevant areas), adaptive dwell time (Cho and Weber 2009), adaptive power level, and special processing in desirable regions of the atmosphere. The characteristics of the hypothetical PAR system that can achieve these capabilities are presented in Weber et al. (2021).

Characterizing turbulence in the PBL is particularly well suited for a PAR as its stationary beam avoids smearing associated with rotating antennas. Hence, both statistical characteristics of motions, including momentum fluxes on scales larger and smaller than the resolution volume, can be estimated more accurately (Xu and Gal-Chen 1993). Variances and covariances at both scales may be useful for inclusion in numerical models or for verifying the models' results. Furthermore, estimates of heat and moisture fluxes from the structure parameter C_n^2 would be useful to numerical models and analysis [Doviak and Zrnić 2006, Eq. (10.38)] profiles; the effect of these fluxes on the reflectivity is illustrated in Rabin and

Doviak (1989). Strength of turbulence can be gauged from measurements of the eddy dissipation rate ε via its relation to the Doppler spectrum width (Doviak and Zrnić 2006).

The S-band radar polarimetric capabilities can distinguish Bragg scatterers (carrier of humidity information) from insects or birds (Melnikov and Zrnić 2017), enabling accurate, uncontaminated measurements of the air motions. We illustrate the concept in Fig. 5 where the vertical cross sections (RHIs) of the differential reflectivity (Z_{DR}) and the copolar correlation coefficient (ρ_{HV}) at the PBL top are displayed for signal to noise ratios larger than −7 dB. The key point is that Z_{DR} and ρ_{HV} at the PBL top (between the two horizontal lines) have distinct values separating Bragg scatter from insects. The Z_{DR} of these eddies is on average zero (Fig. 5a) and the correlation coefficient is close to one (Fig. 5b).

A definite advantage of a PAR for this application is its adaptive increase in sensitivity to detect the weak signals and avoidance of beam smearing effects in the measurements of turbulence. Finally, a broad topic ready for exploration is the use of bistatic measurements in clear air (Tulu et al. 2006) with a PAR wherein the tracers are fluctuations of refractive index. These measurements would sense eddies significantly larger than half the radar wavelength size causing returns in the monostatic application. Larger eddies are more likely to be within the inertial subrange and thus be more detectable.

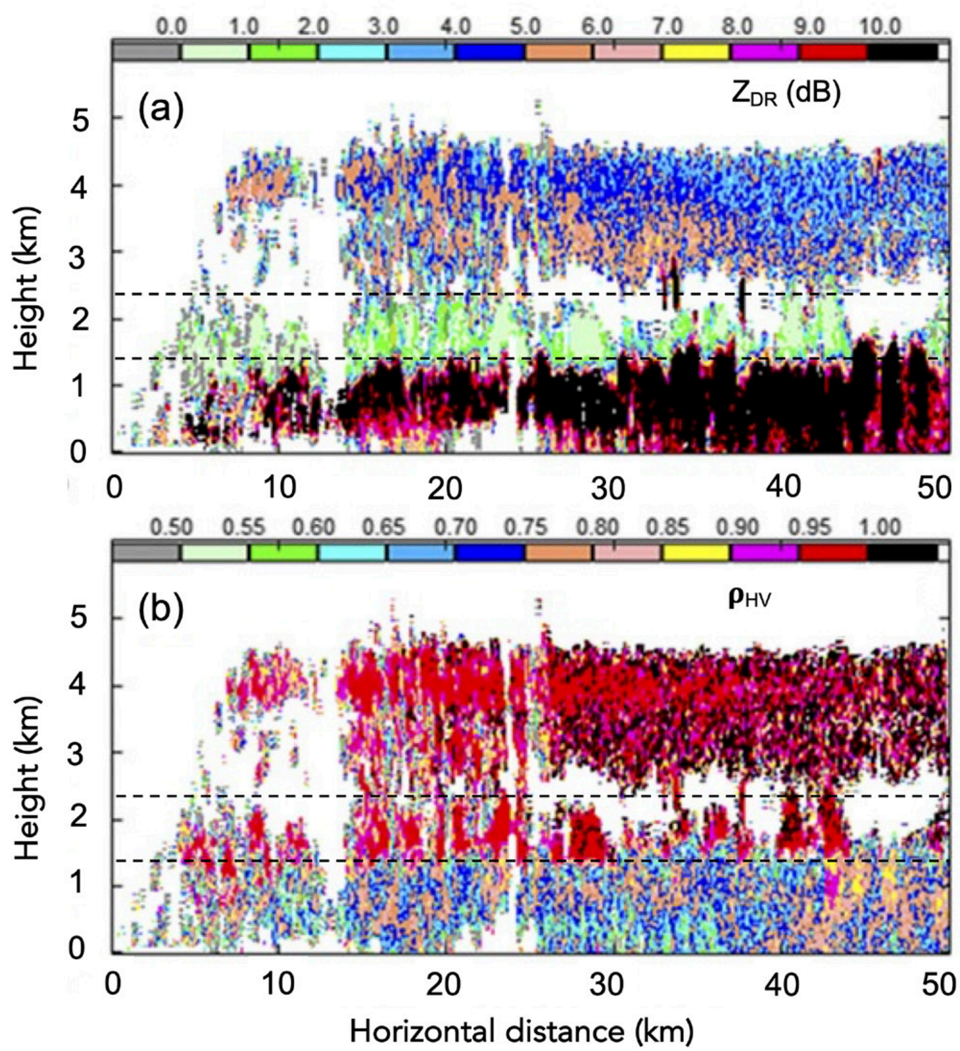

Fig. 5. (a) Vertical cross section (RHI) of differential reflectivity Z_{DR}. (b) Correlation coefficient ρ_{hv} of the data in (a). Time is 1800 UTC 18 Jul 2013 at an azimuth of 191°. The horizontal lines bound the area of clear air echoes at the top of the convective boundary layer. The data were collected by the S-band research KOUN Weather Surveillance Radar-1988 Doppler (WSR-88D) located in Norman, OK (adapted from Melnikov and Zrnić 2017).

Integration with other observing systems and numerical weather prediction models

Symbiosis with reflector radars and integration with other observing systems. The strength of synergistic (multisensor) observations for the study of clouds and precipitation systems is well documented. Two noteworthy examples are the National Aeronautics and Space Administration (NASA) A-Train satellite constellation (Stephens et al. 2018) and the U.S. Department of Energy (DOE) Atmospheric Radiation Measurement (ARM) observatories (Turner and Ellingson 2017). Coordinating multifrequency radar observations are key to covering the wide range of occurring cloud and precipitation conditions and to reinforcing our ability to interpret the radar measurements (Kollias et al. 2020a). Traditionally, the value of multisensor observations emerges long after their collection during a postprocessing phase. Unfortunately, any knowledge gained at that stage is often too late to adjust and optimize the observing strategy, often leaving an incomplete picture of the studied phenomena.

PARs offer substantial improvements in our observing capabilities through augmentation with existing and future observing systems. PARs have indeed been operated side-by-side with reflector-based radars. In most cases, the objective has been to use the polarimetric capability of mechanical scanning radars to evaluate and calibrate the PAR polarimetric observables (Heberling and Frasier 2021). Recently, the synergy between PAR and mechanically scanning radars for scientific investigations was demonstrated at the Stony Brook University–Brookhaven National Laboratory Radar Observatory (SBRO). The observations of a high-quality, Ka-band Scanning Polarimetric Radar (KASPR; Kumjian et al. 2020; Oue et al. 2021) and an X-band dual-polarization phased array radar (SKYLER; Kollias et al. 2018)—two different yet uniquely complementary systems—were adaptively coordinated using real-time observations from a geostationary satellite, a surface camera, and the radars themselves (Kollias et al. 2020b). The high sensitivity and polarimetric quality of the mechanically scanning KASPR, dedicated to a slow scan rate, produced high-quality observations of a series of waterspouts while the agile phased-array SKYLER, in concert, instantaneously interrogated many different parts of the waterspouts to provide missing dynamical context. This combination of radar resources has the potential to provide a leap forward in our ability to understand rapidly evolving microphysical and dynamical processes in cloud and precipitation systems.

Integration with ML/AI-based intelligent observing systems. Only a few scanning radars systematically adapt their sampling strategy based on the actual atmospheric state. An example of this is the Collaborative Adaptive Sensing of the Atmosphere (CASA) network (McLaughlin et al. 2009); a network of small, low-cost, short-range radars controlled by a software architecture, which automatically balances user preferences for information, data quality, system resources, and the evolving weather. Most of our observing systems (i.e., DOE ARM observatories) sample the atmosphere using a predetermined "stare" or "sit and spin" strategy that is not adaptive to atmospheric conditions. This inflexible approach is based on sampling all the sky equally, even clear skies without any atmospheric phenomena of interest. This precludes our ability to selectively sample more frequently in time and with higher spatial resolution the parts of the sky where a particular phenomenon exists.

To truly capitalize on the benefits of an inertia-free beam requires a break from the sit-and-spin style notions of preplanned PPIs, RHIs, and raster scans. By way of analogy, the human visual system offers an example of highly adept, externally driven, dynamic remote sensing (Fig. 6a). The area of the human retina capable of resolving high-resolution images (the fovea, measuring about 1.5 mm across) is a mere fraction of the total retinal area. Its very narrow field of view requires there to be a time-sharing scheme in which the eyes' positions shift rapidly (using saccadic motions) between different features of interest, with

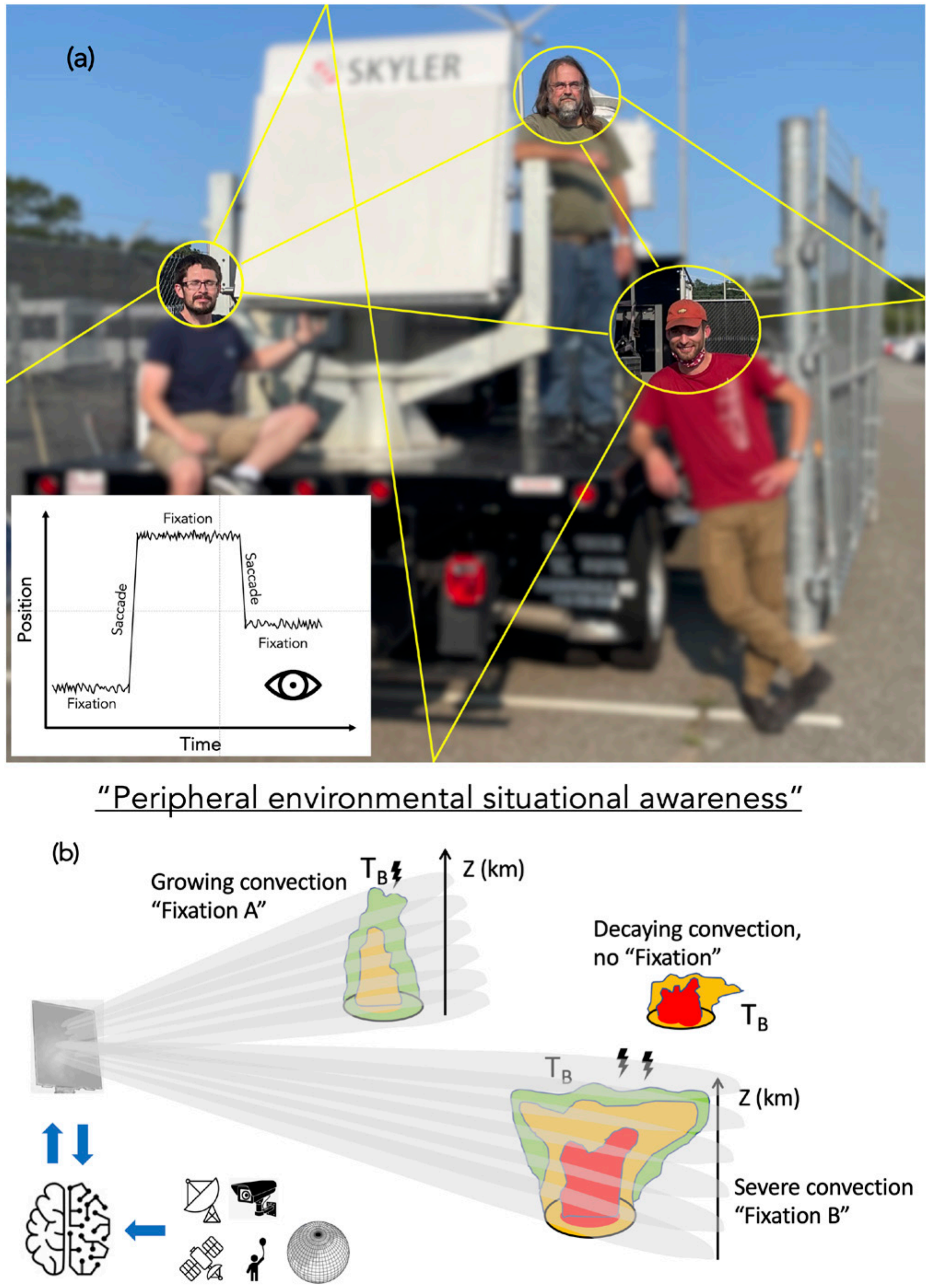

Fig. 6. (a) Example of the regions of high-resolution fixation (yellow circles) where a human observer might spend most of the time aiming the eyes' foveae when viewing this image. The yellow lines represent quick saccadic motions between the fixation points, or analogously, processing overhead of the Saccadic Phased Array Radar Sampling (SPARS) algorithm. The blurred areas represent information content less relevant to the observer. (b) An analogous framework of PAR plus other sensors in an observational network where peripheral environmental situation awareness is provided by a rich multisensor real-time data stream and the fovea-like PAR system spends most of the time directing beams having high-quality SNR toward features of maximum interest. The individuals in (a) are Kristofer Tuftedal (left), Edward Luke (top), and Miles Litzmann (right).

the features containing more important information getting more revisit time (Yarbus 1967). These "snapshots" are then linked together by the brain to extract meaning.

We envision a similar approach for observing convective weather with analogous characteristics, consisting of two parts (Kollias et al. 2022). The first part consists of a very fast ongoing raster scan that blankets the full observational sector in azimuth and elevation with a coarse grid of short dwell-time beams. Every few seconds, all data from the grid are periodically ranked and sorted by descending relevance according to a "goodness metric" to identify the most interesting beam directions. Simultaneously, the second part of our approach targets a set of high spatial resolution longer-dwell beams, prioritizing the directions that were found most relevant, until available beam time is exhausted. The budgeting of beam time is split ~20%/80% by interleaving the first and second parts, allowing high-resolution sampling to be continuously targeted toward the most interesting features as they evolve (Fig. 6b). The first part performs a function analogous to the rods in the human visual system covering the bulk of the optical field and providing peripheral vision. The second part is analogous to the high-resolution fovea that resolves the most interesting content. One important difference in our case is that the "fovea" can assume an arbitrary shape and even split into multiple "foveae," as needed.

Recently, the first iteration of an intelligent agent for weather radars that uses multisensory input for agile adaptive sensing was developed and its evolution from an observing system into an intelligent observing protocol system was demonstrated (Kollias et al. 2020b). The intelligent agent, called Multisensor Agile Adaptive Sampling (MAAS), integrates the ecosystem of existing infrastructure sensing systems [e.g., cameras, satellites (GOES), radars (WSR-88D), lidars] into an artificial intelligence system that can identify phenomena of interest, allocate resources for their tracking and sampling, and creation of the proper warning/response output. MAAS expands upon past efforts (McLaughlin et al. 2009; Stein et al. 2015) by integrating a PAR system and nonradar observations in the determination of the "goodness metric." Projecting this approach further, as phased-array radar becomes integrated with machine learning capabilities, it becomes the input sensor (or eyes, so to speak) of an intelligent atmospheric computer vision system.

Assimilation of PAR data into high-resolution NWP. Another potential utilization of PAR data are through its integration with the Warn-on-Forecast project, a National Oceanic and Atmospheric Administration research initiative that aims to increase lead time for tornado, severe thunderstorm, and flash flood warnings (Stensrud et al. 2013). A major focus of the Warn-on-Forecast initiative is the cycled data assimilation (DA) of PAR reflectivity and/or radial velocity (Lu and Xu 2009; Thompson and Wicker 2009; Yussouf and Stensrud 2010; Wicker et al. 2012; Cheng et al. 2014; Skinner et al. 2014; Tanamachi et al. 2015; Supinie et al. 2017; Stratman et al. 2020; Kerr and Wang 2020; Huang et al. 2020) for short-fuse severe weather prediction.

The nowcasting/detection of severe weather hazards using operational scanning radars is limited by the volume coverage pattern (VCP). This has motivated the development of the SAILS (Supplemental Adaptive Intravolume Low-Level Scan) scanning strategy (Chrisman 2013, 2014), giving more frequent low-level updates in operational WSR-88D data. These adaptive low-level scanning procedures, adding low-level scans to the middle of a VCP, have led to the increased detection of low-level features of interest with a positive influence on severe weather warnings in the United States (Cho et al. 2021; Kingfield and French 2022). However, even with 2–3-min scan updates provided by SAILS, the evolution of convective storm features may still not be resolved, both in time and in the vertical plane.

PAR data have revealed that the evolution of convective storm features can occur on time scales more rapidly than provided by SAILS-type scanning, at more than one scan level, and above low-level scanning. Tornadic vortex signatures (TVSs) scanned by phased-array radars undergo rapid evolution on time scales less than 20 s (e.g., French et al. 2014), such that SAILS-type scanning can alias key variability in observing the tornadic vortex evolution, or the detection and evolution of the tornadic debris signature (TDS) in copolar correlation coefficient (e.g., Houser et al. 2016). For hail nowcasting, features such as specific differential phase and differential phase columns (e.g., Illingworth et al. 1987; Hubbert et al. 1998) may be missed more frequently with enhanced low-level scanning, and the time resolution of operational VCPs may be insufficient for gathering information for hail and severe wind nowcasting algorithms (French and Kingfield 2021; Kingfield and French 2022; Hermes et al. 1993).

PARs flexible scanning capabilities allow "adaptive sampling" or "targeted observations" (Kerr and Wang 2020), providing faster updates in regions of high interest or longer dwells in areas where clear-air returns are desired (Huang et al. 2020, 2022). PAR therefore enables DA to provide accurate high-resolution analysis of both the storm and the near-storm wind field, which is critical for subsequent prediction. Such capabilities also allow DA methods to address model–data imbalance (Maejima et al. 2017), treatment of nonlinearity and non-Gaussianity (e.g., van Leeuwen 2009), and new multiscale DA approaches (e.g., Wang et al. 2021). PARs adaptive sampling capability also opens doors for new research on developing observation operators and observation error estimation models associated with different sampling strategies (e.g., beam patterns).

Given the wealth of information available from polarimetry, assimilation of dual-polarization PAR data into NWP models has the potential to improve the analysis of the storm. Despite this promising avenue, efforts toward even conventional dual-polarization data assimilation have been somewhat limited (Li et al. 2017; Carlin et al. 2017; Putnam et al. 2019), in part because of two roadblocks. First, conventional dual-pol observations are limited in the spatiotemporal resolution needed for high-resolution NWP models. For example, Carlin et al. (2017) show the utility of assimilating Z_{DR} or K_{DP} columns (Kumjian et al. 2014; van Lier-Walqui et al. 2016) to improve storm spinup and forecasts in NWP models. However, poor operational sampling of the mid- and upper levels of storms, exacerbated by the recent focus on more frequent updates at low levels at the expense of midlevel scans (e.g., Kingfield and French 2022) limits the information available for DA. Polarimetric PAR will close these gaps, allowing rapid, comprehensive sampling of convective storms throughout their life cycle, providing critical information for DA. Second, the mismatch between radar-observed quantities (like Z, Z_{DR}, K_{DP}) and model-predicted variables necessitates the design of forward operators (e.g., Ryzhkov et al. 2011; Oue et al. 2020). These are underinformed by model microphysics schemes and require assumptions—sometimes arbitrary—to fill these gaps (Kumjian et al. 2019). As forward operators are developed to be savvier to the uncertainty brought on by this incomplete information (e.g., Schrom and Kumjian 2019) and model microphysics schemes improve (e.g., Morrison et al. 2020), the rich information available from polarimetric PAR will contribute to improved analyses and forecasts of hazardous weather.

How do we make PAR accessible to the community?

The potential scientific gains enumerated above can only be realized with widespread community access to PAR technology. Additionally, dual-polarized PAR is a candidate technology for eventual replacement of the WSR-88D (Weber et al. 2021). Therefore, it is imperative that atmospheric scientists at all career stages, from students to mature researchers, have ample opportunities to interact with, operate, and experiment with PARs. Community PAR access will accelerate the adoption of the technology, ensure educational equity, and prepare students for the future meteorology work force. Some recommendations for how to make PARs more accessible to the radar meteorology, cloud physics, mesoscale meteorology, hydrometeorology, and storm-scale numerical weather prediction communities are described below.

National facility. The scientific community has strongly advocated for the development and use of PAR technology in atmospheric science research (National Research Council 2002; Bluestein et al. 2014; Geerts et al. 2018, 2018). Presently, different research groups have mobile C- and X-band PARs (Kollias et al. 2018, 2020b, 2022; Salazar et al. 2019;

Heberling and Frasier 2021), including dual-polarization capability, that have participated in field experiments. While many PARs exist within the scientific community, it is desirable that the investigators can equitably request PAR systems for a diverse spectrum of research and educational activities through the NSF. PAR technology has largely been used to study severe thunderstorms, but an array of other potential applications exists for studies of microphysical and dynamic processes or boundary layer meteorology. In addition, new PAR technology may be required to maximize scientific impact and address different atmospheric science research areas (e.g., mitigating attenuation using S band or observing clouds using Ka or W bands).

In addition to a ground-based PAR facility, there is a necessity for an airborne PAR system to sample storms in remote regions unreachable by ground-based radars. A large portion of high-impact weather systems (e.g., tropical cyclones, extratropical cyclones, orographic precipitation) have their origins over the oceans or mountainous regions. The National Center for Atmospheric Research (NCAR) has been advocating for an airborne PAR (APAR; Vivekanandan et al. 2020) that can be mounted on the fuselage of an aircraft that expands the potential pool of airborne weather radar platforms onto C-130 and other large fuselage airplanes. Collecting concurrent dual-Doppler and dual-polarization measurements in the interior of storms enables the investigation of the coupling of dynamics and microphysics that fundamentally underlies weather and global climate systems.

Increase the participation of PAR systems in large field experiments. A wide range of atmospheric research can benefit from rapid and adaptive PAR scanning, including shallow/deep convection, convective initiation and updraft dynamics, microphysics, severe storms, tropical cyclones, impact of complex terrain on precipitation processes, and fire weather. Future field campaigns using PAR should be designed by integrating multiple PARs and instruments (e.g., lidars, aircraft measurements), and their deployments should be optimized prior to field campaigns using numerical models and radar simulators (Oue et al. 2019; Mahre et al. 2018; Torres and Schvartzman 2020). Deployment of at least two PARs is critical for multi-Doppler, three-dimensional wind retrievals. For example, multiple PARs could be used simultaneously to adaptively scan boundary layer and convection initiation processes while documenting vertical motions and microphysical processes in mature, deep convection. Precipitation processes and rapidly evolving dynamics could be explored near coastal transitions for lake/sea-effect snow, to understand the influence of complex terrain, or to capture sea-breeze initiated convection. To ensure high data quality, existing validation and visualization tools should be effectively used to quantify uncertainties in the observations, including direct comparisons between reflector antenna and PAR data during field campaigns. Intercomparisons of dual-polarization data and PAR data collected in nontraditional scanning modes (e.g., imaging) with dish systems will help the scientific community to use and gain confidence in PAR system capabilities. PAR systems should also be made available for education and exploratory research requests to provide critical training with state-of-the-art radar technologies and facilitate the availability of a PAR system to institutions that traditionally could not afford or support a system of their own.

Future workshop, conferences, and open data access. The organization of a future workshop that focuses specifically on PARs to broaden the potential applications and user-base of this technology is recommended. The workshop can be sponsored by NSF and other agencies such as the DOE and NASA. That guidance will help fine-tune PAR operations needs and address limitations in accessibility.

To promote PAR abilities with the goal of this broader accessibility, PAR scientists need to present at specialty conferences that reach beyond the radar community to include boundary layer, mesoscale, and hydrology groups, for example. This increased awareness of PAR systems and applications will facilitate the development of accessible datasets and software for broader uses. To date, PAR datasets have primarily focused on severe storms, have lacked polarimetric capability, and in some cases are difficult to broadly share due to the constraints imposed by funding sources. To make data more broadly accessible, an important goal for this community is to create a more diverse collection of PAR datasets with existing systems and make past datasets accessible.

Another important dimension of the proposed strategy to increase PAR accessibility to the community is to develop a consistently documented, centrally located database of PAR cases. To foster community-wide access to PAR data, a centralized data repository is needed (e.g., through the Earth Observing Laboratory) as well as the adaptation of community analysis and visualization tools through open-source software frameworks. Future efforts will then include a diverse set of voices from the operational, research, and educational communities to develop best practices and a consistent framework for improving accessibility of PAR data.

Epilogue

PAR capabilities are expected to substantially improve our ability to develop agile, adaptive observing systems that will provide higher spatiotemporal resolution and allow us to document the entire life cycle of cloud and precipitation systems.

PAR-enabled quantitative process rate information in precipitation will be a major step forward in evaluating model microphysical parameterizations. With improved spatiotemporal continuity, long-standing sampling gaps will be addressed by enabling a near-4D depiction of microphysical processes with full volume scans collected in <1 min, benefiting NWP modeling, data assimilation, and bringing broad impacts to related disciplines like hydrology. Future research should include PAR observations with the dual-polarization capability, in conjunction with in situ thermodynamic measurements and numerical modeling, to improve our scientific knowledge and warning technology of relatively compact yet severe events.

To truly utilize the PARs capabilities in atmospheric sciences, we need to integrate them into a machine learning (ML)/artificial intelligence (AI)-based, data-driven, dynamic observing framework (Kollias et al. 2020b, 2022). A rich data ecosystem with inputs from both PAR and non-PAR observations (i.e., GOES, surface cameras, WSR-88D) can be synthesized by a machine learning system into a more holistic description of the atmospheric state, creating best-estimate positional guidance for real-time tracking by surface-based sensors, and developing a better understanding of the fundamental physics.

Here, we purposely avoided making recommendations toward the ongoing debate surrounding the next-generation operational weather radar network in the United States and whether it should be based exclusively on PAR technology or a hybrid network of reflector-based radars and PARs. The purpose of the article is to pivot the PAR discussion that, to date, has been dominated by the ongoing debate surrounding the potential of PARs to replace the current U.S. operational weather radar network (WSR-88D). The significant research and development focused on this topic is expected to improve PAR capabilities across the board (research and operational systems), while the parallel discussion on PAR capabilities and applications is mostly limited to the operational requirements of the NWS and NOAA. These requirements were designed to improve weather warning and forecasting capabilities with a particular technology and capability in hand (reflector-based radars).

It is not clear whether many of these requirements are directly applicable to PARs. Throughout the article we highlight the PAR's transformative capabilities and its potential to revolutionize the way we observe weather. For example, what is the relevance of the concept of a temporal update cycle for a PAR? PARs challenge the current paradigm where "the radar sampling time is equally divided across all parts of the atmosphere." It is plausible that PARs can match, and probably improve by up to a factor of 5, the time it takes for a WSR-88D to cover the same VCP (effectively by avoiding sectors with no meteorological echoes or by using adaptive scanning modes such as imaging) but at the same time, the same PAR system can sample selected convective storms with superior vertical resolution using densely oversampled elevation beams. Similarly, is the antenna beamwidth the best parameter to characterize the radar angular resolution when one system (PAR) can conduct any desirable oversampling in azimuth and elevation while staring, and the other (reflector-based radar) is rotating while sampling? One is left to wonder whether such measurement requirements would have been necessary if PAR was the original technology and capability at hand.

Finally, our experience working with research-grade PARs for the past 5–10 years illustrate there is much more to discuss and benefit from PARs, even if they do not exactly meet the current NOAA/NWS requirements. Here, our aim was to communicate these benefits to the broader research community, increase the number of early adopters, and thus create a research community that actively conducts research using PARs.

Acknowledgments. PK contributions were supported by Contract DE-SC0012704 with the U.S. Department of Energy (DOE) and NSF Grant AGS-2019932. MO contributions were supported by the DE-SC02211160 and NSF Grant AGS-2019932. TA contributions were supported by JSPS KAKENHI Grants JP17K13007 and JP21K03666. RP, DB, and JS contributions were supported by the NOAA/Office of Oceanic and Atmospheric Research under NOAA–University of Oklahoma Cooperative Agreement NA21OAR4320204. DB was also supported by NSF Grant AGS-2114817. JMK and JYNC contributions were supported by the United States Air Force under Air Force Contract FA8702-15-D-0001. RT contributions were supported by NSF Grant AGS-1741003. SN contributions were supported by NSF Grant AGS-2113207. XW contributions were supported by NA160AR4320115. HB contributions were supported by NSF AGS-1947146. EPL contributions were supported by Contract DE-SC0012704. PEK contributions were supported by NA21OAR4320204 and NASA's Precipitation Measurement Mission Award 80NSSC19K0681 and 80NSSC21K2045. MK contributions were supported by NSF Grant AGS-2020000. Any opinions, findings, conclusions, or recommendations expressed in this material are those of the authors and do not necessarily reflect the views of the sponsoring organizations.

Data availability statement. Several high-resolution datasets are available at the ARRC https://arrc.ou.edu/data.html and SBRO http://radarscience.weebly.com data portals.

References

Adachi, T., and W. Mashiko, 2020: High temporal-spatial resolution observation of tornadogenesis in a shallow supercell associated with Typhoon Hagibis (2019) using phased array weather radar. *Geophys. Res. Lett.*, **47**, e2020GL089635, https://doi.org/10.1029/2020GL089635.

Andrić, J., M. R. Kumjian, D. S. Zrnić, J. Straka, and V. Melnikov, 2013: Polarimetric signatures above the melting layer in winter storms: An observational and modeling study. *J. Appl. Meteor. Climatol.*, **52**, 682–700, https://doi.org/10.1175/JAMC-D-12-028.1.

Bachmann, S. M., and D. S. Zrnić, 2007: Spectral density of polarimetric variables separating biological scatterers in the VAD display. *J. Atmos. Oceanic Technol.*, **24**, 1186–1198, https://doi.org/10.1175/JTECH2043.1.

Bluestein, H. B., M. M. French, I. PopStefanija, R. T. Bluth, and J. B. Knorr, 2010: A mobile, phased-array Doppler radar for the study of severe convective storms: The MWR-05XP. *Bull. Amer. Meteor. Soc.*, **91**, 579–600, https://doi.org/10.1175/2009BAMS2914.1.

——, and Coauthors, 2014: Radar in atmospheric sciences and related research: Current systems, emerging technology, and future needs. *Bull. Amer. Meteor. Soc.*, **95**, 1850–1861, https://doi.org/10.1175/BAMS-D-13-00079.1.

——, J. C. Snyder, and J. B. Houser, 2015: A multi-scale overview of the El Reno, Oklahoma tornadic supercell of 31 May 2013. *Wea. Forecasting*, **30**, 525–552, https://doi.org/10.1175/WAF-D-14-00152.1.

——, M. M. French, J. C. Snyder, and J. B. Houser, 2016: Doppler radar observations of anticyclonic tornadoes in cyclonically rotating, right-moving supercells. *Mon. Wea. Rev.*, **144**, 1591–1616, https://doi.org/10.1175/MWR-D-15-0304.1.

——, K. J. Thiem, J. C. Snyder, and J. B. Houser, 2018: The multiple-vortex structure of the El Reno, Oklahoma, tornado on 31 May 2013. *Mon. Wea. Rev.*, **146**, 2483–2502, https://doi.org/10.1175/MWR-D-18-0073.1.

——, ——, ——, and ——, 2019a: Tornadogenesis and early tornado evolution in the El Reno, Oklahoma, supercell on 31 May 2013. *Mon. Wea. Rev.*, **147**, 2045–2066, https://doi.org/10.1175/MWR-D-18-0338.1.

——, D. T. Lindsey, D. Bikos, D. W. Reif, and Z. B. Wienhoff, 2019b: The relationship between overshooting tops in a tornadic supercell and its radar-observed evolution. *Mon. Wea. Rev.*, **147**, 4151–4176, https://doi.org/10.1175/MWR-D-19-0159.1.

Bodine, D., R. Palmer, P. Kirstetter, T.-Y. Yu, M. Yeary, and C. Fulton, 2021: Virtual workshop on atmospheric science applications of ground based phased array radars. Workshop Rep., 30 pp., https://arrc.ou.edu/pdf/2021-PAR-Workshop-Report.pdf.

Bousquet, O., P. Tabary, and J. Parent du Châtelet, 2007: On the value of operationally synthesized multiple-Doppler wind fields. *Geophys. Res. Lett.*, **34**, L22813, https://doi.org/10.1029/2007GL030464.

Bringi, V. N., and V. Chandrasekar, 2001: *Polarimetric Doppler Weather Radar: Principles and Applications.* Cambridge University Press, 664 pp., https://doi.org/10.1017/CBO9780511541094.

Brookner, E., 1985: Phased-array radars. *Sci. Amer.*, **252**, 94–102, https://doi.org/10.1038/scientificamerican0285-94.

Bukovcic, P., A. Ryzhkov, and D. Zrnić, 2020: Polarimetric relations for snow estimation radar verification. *J. Appl. Meteor. Climatol.*, **59**, 991–1009, https://doi.org/10.1175/JAMC-D-19-0140.1.

Byrne, D., and J. A. Zhang, 2013: Height-dependent transition from 3-D to 2-D turbulence in the hurricane boundary layer. *Geophys. Res. Lett.*, **40**, 1439–1442, https://doi.org/10.1002/grl.50335.

Carlin, J. T., J. Gao, J. C. Snyder, and A. Ryzhkov, 2017: Assimilation of Z_{DR} columns for improving the spinup and forecast of convective storms in storm-scale models: Proof-of-concept experiments. *Mon. Wea. Rev.*, **145**, 5033–5057, https://doi.org/10.1175/MWR-D-17-0103.1.

Cheng, J., N. Yussouf, Y. Jung, D. J. Stensrud, M. Xue, and L. J. Wicker, 2014: Impact of phased array radar observations on the analyses and forecasts of the 22 May 2011 Ada supercell storm. *27th Conf. on Severe Local Storms*, Madison, Wisconsin, Amer. Meteor. Soc., 12A.5, https://ams.confex.com/ams/27SLS/webprogram/Paper255283.html.

Cho, J. Y. N., and M. Weber, 2009: MPAR characteristics and potential service improvements. *Second National Symp. on Multifunction Phased Array Radar*, Norman, OK, ICAMS, 4.2, www.icams-portal.gov/resources/ofcm/groups/mpar/meetings/symposium/Session04/S42_Cho-MPAR2-Session4.pdf.

——, B. E. Anderson, J. D. W. Barrick, and K. L. Thornhill, 2001: Aircraft observations of boundary layer turbulence: Intermittency and the cascade of energy and passive scalar variance. *J. Geophys. Res.*, **106**, 32 469–32 479, https://doi.org/10.1029/2001JD900079.

——, J. M. Kurdzo, and B. J. Bennett, 2021: Impact of WSR-88D SAILS usage on NWS severe weather warning performance. *37th Conf. on Environmental Information Processing Technologies*, Online, Amer. Meteor. Soc., 10.5, https://ams.confex.com/ams/101ANNUAL/meetingapp.cgi/Paper/378933.

Chrisman, J. N., 2013: Dynamic scanning. *NEXRAD Now*, No. 22, NOAA/Radar Operations Center, Norman, OK, 1–3, www.roc.noaa.gov/WSR88D/PublicDocs/NNOW/NNow22c.pdf.

——, 2014: Multiple elevation scan option for SAILS (MESO-SAILS)—The next step in dynamic scanning for the WSR-88D. Radar Operations Center, 27 pp., www.roc.noaa.gov/wsr88d/PublicDocs/NewTechnology/MESO-SAILS_Description_Briefing_Jan_2014.pdf.

Doviak, R., and D. Zrnić, 2006: *Doppler Radar and Weather Observations.* 2nd ed. Dover, 562 pp.

Fabry, F., 2015: *Radar Meteorology: Principles and Practice.* Cambridge University Press, 277 pp., https://doi.org/10.1017/CBO9781107707405.

French, M. M., and D. M. Kingfield, 2021: Tornado formation and intensity prediction using polarimetric radar estimates of updraft area. *Wea. Forecasting*, **36**, 2211–2231, https://doi.org/10.1175/WAF-D-21-0087.1.

——, H. B. Bluestein, I. PopStefanija, C. A. Baldi, and R. T. Bluth, 2013: Reexamining the vertical development of descending tornadic vortex signatures in supercells. *Mon. Wea. Rev.*, **136**, 4576–4601, https://doi.org/10.1175/MWR-D-12-00315.1.

——, H. Bluestein, I. PopStefanija, C. A. Baldi, and R. T. Bluth, 2014: Mobile, phased-array, Doppler radar observations of tornadoes at X band. *Mon. Wea. Rev.*, **142**, 1010–1036, https://doi.org/10.1175/MWR-D-13-00101.1.

Fridlind, A. M., and Coauthors, 2019: Use of polarimetric radar measurements to constrain simulated convective cell evolution: A pilot study with Lagrangian tracking. *Atmos. Meas. Tech.*, **12**, 2979–3000, https://doi.org/10.5194/amt-12-2979-2019.

Geerts, B., and Coauthors, 2018: Recommendations for in-situ and remote sensing capabilities in atmospheric convection and turbulence. *Bull. Amer. Meteor. Soc.*, **99**, 2463–2470, https://doi.org/10.1175/BAMS-D-17-0310.1.

Gossard, E. E., R. B. Chadwick, W. S. Neff, and K. P. Moran, 1982: The use of ground-based Doppler radars to measure gradients, fluxes and structure parameters in elevated layers. *J. Appl. Meteor.*, **21**, 211–226, https://doi.org/10.1175/1520-0450(1982)021<0211:TUOGBD>2.0.CO;2.

Grabowski, W. W., and H. Morrison, 2021: Supersaturation, buoyancy, and deep convective dynamics. *Atmos. Chem. Phys.*, **21**, 13 997–14 018, https://doi.org/10.5194/acp-21-13997-2021.

Griffin, E. M., T. J. Schuur, and A. V. Ryzhkov, 2018: A polarimetric analysis of ice microphysical processes in snow, using quasi-vertical profiles. *J. Appl. Meteor. Climatol.*, **57**, 31–50, https://doi.org/10.1175/JAMC-D-17-0033.1.

Heberling, W., and S. J. Frasier, 2021: On the projection of polarimetric variables observed by a planar phased-array radar at X-band. *IEEE Trans. Geosci. Remote Sens.*, **59**, 3891–3903, https://doi.org/10.1109/TGRS.2020.3023640.

Heinselman, P. L., and S. M. Torres, 2011: High-temporal-resolution capabilities of the National Weather Radar Testbed Phased-Array Radar. *J. Appl. Meteor. Climatol.*, **50**, 579–593, https://doi.org/10.1175/2010JAMC2588.1.

——, D. J. Stensrud, R. M. Hluchan, P. L. Spencer, P. C. Burke, and K. L. Elmore, 2009: Radar reflectivity–based estimates of mixed layer depth. *J. Atmos. Oceanic Technol.*, **26**, 229–239, https://doi.org/10.1175/2008JTECHA1091.1.

Hermes, L. G., A. Witt, S. D. Smith, D. Klingle-Wilson, D. Morris, G. J. Stumpf, and M. D. Eilts, 1993: The gust-front detection and wind-shift algorithms for the terminal Doppler weather radar system. *J. Atmos. Oceanic Technol.*, **10**, 693–709, https://doi.org/10.1175/1520-0426(1993)010<0693:TGFDAW>2.0.CO;2.

Houser, J. B., H. B. Bluestein, and J. C. Snyder, 2015: Rapid-scan, polarimetric, Doppler radar observations of tornadogenesis and tornado dissipation in a tornadic supercell: The "El Reno, Oklahoma" storm of 24 May 2011. *Mon. Wea. Rev.*, **143**, 2685–2710, https://doi.org/10.1175/MWR-D-14-00253.1.

——, N. McGinnis, K. M. Butler, H. B. Bluestein, J. C. Snyder, and M. M. French, 2020: Statistical and empirical relationships between tornado intensity and both topography and land cover using rapid-scan radar observations and a GIS. *Mon. Wea. Rev.*, **148**, 4313–4338, https://doi.org/10.1175/MWR-D-19-0407.1.

Houser, J. L., H. B. Bluestein, and J. C. Snyder, 2016: A finescale radar examination of the tornadic debris signature and weak-echo reflectivity band associated with a large, violent tornado. *Mon. Wea. Rev.*, **144**, 4101–4130, https://doi.org/10.1175/MWR-D-15-0408.1.

Huang, Y., X. Wang, C. Kerr, A. Mahre, T. Yu, and D. Bodine, 2020: Impact of assimilating clear-air radial velocity observations from phased array radar on the forecasting of supercell thunderstorm: An observing system simulation experiment study. *Mon. Wea. Rev.*, **148**, 3825–3845, https://doi.org/10.1175/MWR-D-19-0391.1.

——, ——, A. Mahre, T.-Y. Yu, and D. Bodine, 2022: Impacts of assimilating future phased array radar clear-air radial velocity observations on convective initiation forecasts. *Mon. Wea. Rev.*, **150**, 1563–1583, https://doi.org/10.1175/MWR-D-21-0199.1.

Hubbert, J., V. N. Bringi, L. D. Carey, and S. Bolen, 1998: CSU-CHILL polarimetric radar measurements from a severe hail storm in eastern Colorado. *J. Appl. Meteor.*, **37**, 749–775, https://doi.org/10.1175/1520-0450(1998)037<0749:CCPRMF>2.0.CO;2.

Igel, A. L., and S. C. van den Heever, 2021: Invigoration or enervation of convective clouds by aerosols? *Geophys. Res. Lett.*, **48**, e2021GL093804, https://doi.org/10.1029/2021GL093804.

Illingworth, A. J., J. W. F. Goddard, and S. M. Cherry, 1987: Polarization radar studies of precipitation development in convective storms. *Quart. J. Roy. Meteor. Soc.*, **113**, 469–489, https://doi.org/10.1002/qj.49711347604.

Junyent, F., V. Chandrasekar, D. McLaughlin, E. Insanic, and N. Bharadwaj, 2010: The CASA Integrated Project 1 networked radar system. *J. Atmos. Oceanic Technol.*, **27**, 61–78, https://doi.org/10.1175/2009JTECHA1296.1.

Kalesse, H., W. Szyrmer, S. Kneifel, P. Kollias, and E. Luke, 2016: Fingerprints of a riming event on cloud radar Doppler spectra: Observations and modeling. *Atmos. Chem. Phys.*, **16**, 2997–3012, https://doi.org/10.5194/acp-16-2997-2016.

Kerr, C. A., and X. Wang, 2020: Ensemble-based targeted observation method applied to radar radial velocity observations on idealized supercell low-level rotation forecasts: A proof of concept. *Mon. Wea. Rev.*, **148**, 877–890, https://doi.org/10.1175/MWR-D-19-0197.1.

Kingfield, D. M., and M. M. French, 2022: The influence of WSR-88D intra-volume scanning strategies on thunderstorm observations and warnings in the dual-polarization radar era: 2011–20. *Wea. Forecasting*, **37**, 283–301, https://doi.org/10.1175/WAF-D-21-0127.1.

Kirstetter, P. E., H. Andrieu, G. Delrieu, and B. Boudevillain, 2010: Identification of vertical profiles of reflectivity for correction of volumetric radar data using rainfall classification. *J. Appl. Meteor. Climatol.*, **49**, 2167–2180, https://doi.org/10.1175/2010JAMC2369.1.

——, ——, B. Boudevillain, and G. Delrieu, 2013: A physically-based identification of vertical profiles of reflectivity from volume scan radar data. *J. Appl. Meteor. Climatol.*, **52**, 1645–1663, https://doi.org/10.1175/JAMC-D-12-0228.1.

Kollias, P., D. J. McLaughlin, S. Frasier, M. Oue, E. Luke, and A. Sneddon, 2018: Advances and applications in low-power phased array X-band weather radars. *2018 IEEE Radar Conf. (RadarConf18)*, Oklahoma City, OK, IEEE, 1359–1364, https://doi.org/10.1109/RADAR.2018.8378762.

——, and Coauthors, 2020a: The ARM radar network: At the leading edge of cloud and precipitation observations. *Bull. Amer. Meteor. Soc.*, **101**, E588–E607, https://doi.org/10.1175/BAMS-D-18-0288.1.

——, E. Luke, M. Oue, and K. Lamer, 2020b: Agile adaptive radar sampling of fast-evolving atmospheric phenomena guided by satellite imagery and surface cameras. *Geophys. Res. Lett.*, **45**, e2020GL088440, https://doi.org/10.1029/2020GL088440.

——, ——, K. Tuftedal, M. Dubois, and E. J. Knapp, 2022: Agile weather observations using a dual-polarization X-band phased array radar. *2022 IEEE Radar Conf*., New York, NY, IEEE, 1–6, https://doi.org/10.1109/RadarConf2248738.2022.9764308.

Kumar, V. V., C. Jakob, A. Protat, C. R. Williams, and P. T. May, 2015: Mass-flux characteristics of tropical cumulus clouds from wind profiler observations at Darwin, Australia. *J. Atmos. Sci.*, **72**, 1837–1855, https://doi.org/10.1175/JAS-D-14-0259.1.

Kumjian, M. R., and A. V. Ryzhkov, 2010: The impact of evaporation on polarimetric characteristics of rain: Theoretical model and practical implications. *J. Appl. Meteor. Climatol.*, **49**, 1247–1267, https://doi.org/10.1175/2010JAMC2243.1.

——, and ——, 2012: The impact of size sorting on the polarimetric radar variables. *J. Atmos. Sci.*, **69**, 2042–2060, https://doi.org/10.1175/JAS-D-11-0125.1.

——, and O. P. Prat, 2014: The impact of raindrop collisional processes on the polarimetric radar variables. *J. Atmos. Sci.*, **71**, 3052–3067, https://doi.org/10.1175/JAS-D-13-0357.1.

——, and K. Lombardo, 2017: Insights into the evolving microphysical and kinematic structure of northeastern U.S. winter storms from dual-polarization Doppler radar. *Mon. Wea. Rev.*, **145**, 1033–1061, https://doi.org/10.1175/MWR-D-15-0451.1.

——, S. M. Ganson, and A. V. Ryzhkov, 2012: Raindrop freezing in deep convective updrafts: A microphysical and polarimetric model. *J. Atmos. Sci.*, **69**, 3471–3490, https://doi.org/10.1175/JAS-D-12-067.1.

——, A. P. Khain, N. Benmoshe, E. Ilotoviz, A. V. Ryzhkov, and V. T. Phillips, 2014: The anatomy and physics of Z_{DR} columns: Investigating a polarimetric radar signature with a spectral bin microphysical model. *J. Appl. Meteor. Climatol.*, **53**, 1820–1843, https://doi.org/10.1175/JAMC-D-13-0354.1.

——, C. P. Martinkus, O. P. Prat, S. Collis, M. van Lier-Walqui, and H. Morrison, 2019: A moment-based polarimetric radar forward operator for rain microphysics. *J. Appl. Meteor. Climatol.*, **58**, 113–130, https://doi.org/10.1175/JAMC-D-18-0121.1.

——, D. Tobin, M. Oue, and P. Kollias, 2020: Microphysical insights into ice pellet formation revealed by fully polarimetric Ka-band Doppler radar. *J. Appl. Meteor. Climatol.*, **59**, 1557–1580, https://doi.org/10.1175/JAMC-D-20-0054.1.

Kurdzo, J. M., and Coauthors, 2017: Observations of severe local storms and tornadoes with the atmospheric imaging radar. *Bull. Amer. Meteor. Soc.*, **98**, 915–935, https://doi.org/10.1175/BAMS-D-15-00266.1.

Laurencin, C. N., A. Didlake, S. Loeffler, M. R. Kumjian, and G. Heymsfield, 2020: Hydrometeor size sorting in the asymmetric eyewall of Hurricane Matthew (2016). *J. Geophys. Res. Atmos.*, **125**, e2020JD032671, https://doi.org/10.1029/2020JD032671.

Lhermitte, R., and L. Miller, 1970: Doppler radar methodology for the observation of convective storms. *14th Conf. on Radar Meteorolgy*, Tuscon, AZ, Amer. Meteor. Soc., 133–138.

Li, X., J. R. Mecikalski, and D. Posselt, 2017: An ice-phase microphysics forward model and preliminary results of polarimetric radar data assimilation. *Mon. Wea. Rev.*, **145**, 683–708, https://doi.org/10.1175/MWR-D-16-0035.1.

Liou, Y. C., H. B. Bluestein, M. M. French, and Z. B. Wienhoff, 2018: Single-Doppler velocity retrieval of the wind field in a tornadic supercell using mobile, phased-array, Doppler radar data. *J. Atmos. Oceanic Technol.*, **35**, 1649–1663, https://doi.org/10.1175/JTECH-D-18-0004.1.

Lu, H., and Q. Xu, 2009: Trade-offs between measurement accuracy and resolutions in configuring phased-array radar velocity scans for ensemble-based storm-scale data assimilation. *J. Appl. Meteor. Climatol.*, **48**, 1230–1244, https://doi.org/10.1175/2008JAMC2009.1.

Maejima, Y., M. Kunii, and T. Miyoshi, 2017: 30-second-update 100-m-mesh data assimilation experiments: A sudden local rain case in Kobe on 11 September 2014. *SOLA*, **13**, 174–180, https://doi.org/10.2151/sola.2017-032.

Mahre, A., J. M. Kurdzo, D. J. Bodine, C. B. Griffin, and R. D. Palmer, 2018: Analysis of the 16 May 2015 Tipton, Oklahoma, EF-3 tornado at high spatiotemporal resolution using the Atmospheric Imaging Radar. *Mon. Wea. Rev.*, **146**, 2103–2124, https://doi.org/10.1175/MWR-D-17-0256.1.

Markowski, P., and Y. Richardson, 2011: *Mesoscale Meteorology in Midlatitudes.* John Wiley & Sons, 432 pp.

Matrosov, S. Y., A. V. Ryzhkov, M. Maahn, and G. de Boer, 2020: Hydrometeor shape variability in snowfall as retrieved from polarimetric radar measurements. *J. Appl. Meteor. Climatol.*, **59**, 1503–1517, https://doi.org/10.1175/JAMC-D-20-0052.1.

McKeown, K. E., M. M. French, K. S. Tuftedal, D. M. Kingfield, H. B. Bluestein, D. W. Reif, and Z. B. Wienhoff, 2020: Rapid-scan and polarimetric radar observations of the dissipation of a violent tornado on 9 May 2016 near Sulphur, Oklahoma, 2020. *Mon. Wea. Rev.*, **148**, 3951–3971, https://doi.org/10.1175/MWR-D-20-0033.1.

McLaughlin, D., and Coauthors, 2009: Short-wavelength technology and the potential for distributed networks of small radar systems. *Bull. Amer. Meteor. Soc.*, **90**, 1797–1818, https://doi.org/10.1175/2009BAMS2507.1.

Melnikov, V., and D. S. Zrnić, 2017: Observations of convective thermals with weather radar. *J. Atmos. Oceanic Technol.*, **34**, 1585–1590, https://doi.org/10.1175/JTECH-D-17-0068.1.

Melnikov, V. M., D. S. Zrnić, R. M. Rabin, and P. Zhang, 2008: Radar polarimetric signatures of fire plumes in Oklahoma. *Geophys. Res. Lett.*, **35**, L14815, https://doi.org/10.1029/2008GL034311.

Morotomi, K., S. Shimamura, F. Kobayashi, T. Takamura, T. Takano, A. Higuchi, and H. Iwashita, 2020: Evolution of a tornado and debris ball associated with Super Typhoon Hagibis 2019 observed by X-band phased array weather radar in Japan. *Geophys. Res. Lett.*, **47**, e2020GL091061, https://doi.org/10.1029/2020GL091061.

Morrison, H., and Coauthors, 2020: Confronting the challenge of modeling cloud and precipitation microphysics. *J. Adv. Model. Earth Syst.*, **12**, e2019MS001689, https://doi.org/10.1029/2019MS001689.

North, K. W., M. Oue, P. Kollias, S. E. Giangrande, S. M. Collis, and C. K. Potvin, 2017: Vertical air motion retrievals in deep convective clouds using the ARM scanning radar network in Oklahoma during MC3E. *Atmos. Meas. Tech.*, **10**, 2785–2806, https://doi.org/10.5194/amt-10-2785-2017.

National Research Council, 2002: *Weather Radar Technology Beyond NEXRAD.* National Academies Press, 97 pp., https://doi.org/10.17226/10394.

Oue, M., M. Kumjian, Y. Lu, J. Verlinde, K. Aydin, and E. Clothiaux, 2015a: Linear depolarization ratios of columnar ice crystals in a deep precipitation system over the Arctic observed by zenith-pointing Ka-band Doppler radar. *J. Appl. Meteor. Climatol.*, **54**, 1060–1068, https://doi.org/10.1175/JAMC-D-15-0012.1.

——, M. R. Kumjian, Y. Lu, Z. Jiang, E. Clothiaux, J. Verlinde, and K. Aydin, 2015b: X-band polarimetric and Ka-band Doppler spectral radar observations of a graupel-producing Arctic mixed-phase cloud. *J. Appl. Meteor. Climatol.*, **54**, 1335–1351, https://doi.org/10.1175/JAMC-D-14-0315.1.

——, P. Kollias, A. Ryzhkov, and E. P. Luke, 2018: Towards exploring the synergy between cloud radar polarimetry and Doppler spectral analysis in deep cold precipitating systems in the Arctic. *J. Geophys. Res. Atmos.*, **123**, 2797–2815, https://doi.org/10.1002/2017JD027717.

——, ——, A. Shapiro, A. Tatarevic, and T. Matsui, 2019: Investigation of observational error sources in multi-Doppler-radar three-dimensional variational vertical air motion retrievals. *Atmos. Meas. Tech.*, **12**, 1999–2018, https://doi.org/10.5194/amt-12-1999-2019.

——, A. Tatarevic, P. Kollias, D. Wang, K. Yu, and A. M. Vogelmann, 2020: The Cloud-resolving model Radar SIMulator (CR-SIM) Version 3.3: Description and applications of a virtual observatory. *Geosci. Model Dev.*, **13**, 1975–1998, https://doi.org/10.5194/gmd-13-1975-2020.

——, ——, S. Y. Matrosov, A. Battaglia, and A. V. Ryzhkov, 2021: Analysis of the microphysical properties of snowfall using scanning polarimetric and vertically pointing multi-frequency Doppler radars. *Atmos. Meas. Tech.*, **14**, 4893–4913, https://doi.org/10.5194/amt-14-4893-2021.

Palmer, R., and Coauthors, 2022: A primer on phased array radar technology for the atmospheric sciences. *Bull. Amer. Meteor. Soc.*, **103**, E2205–2230, https://doi.org/10.1175/BAMS-D-21-0172.1.

Pazmany, A. L., J. B. Mead, H. B. Bluestein, J. C. Snyder, and J. B. Houser, 2013: A mobile, rapid-scanning, X-band, polarimetric (RaXPol) Doppler radar system. *J. Atmos. Oceanic Technol.*, **30**, 1398–1413, https://doi.org/10.1175/JTECH-D-12-00166.1.

Peters, J. M., H. Morrison, G. J. Zhang, and S. W. Powell, 2021: Improving the physical basis for updraft dynamics in deep convection parameterizations. *J. Adv. Model. Earth Syst.*, **13**, e2020MS002282, https://doi.org/10.1029/2020MS002282.

Porcacchia, L., P. E. Kirstetter, V. Maggioni, and S. Tanelli, 2019: Investigating the space-borne radar signatures of coalescence dominant precipitation. *Quart. J. Roy. Meteor. Soc.*, **145**, 3161–3174, https://doi.org/10.1002/qj.3611.

Potter, S., 2007: Fine-tuning Fujita. *Weatherwise*, **60**, 64–71, https://doi.org/10.3200/WEWI.60.2.64-71.

Potvin, C. K., L. J. Wicker, and A. Shapiro, 2012: Assessing errors in variational dual-Doppler wind syntheses of supercell thunderstorms observed by storm-scale mobile radars. *J. Atmos. Oceanic Technol.*, **29**, 1009–1025, https://doi.org/10.1175/JTECH-D-11-00177.1.

Protat, A., and I. Zawadzki, 1999: A variational method for real-time retrieval of three-dimensional wind field from multiple-Doppler bistatic radar network data. *J. Atmos. Oceanic Technol.*, **16**, 432–449, https://doi.org/10.1175/1520-0426(1999)016<0432:AVMFRT>2.0.CO;2.

Putnam, B., M. Xue, Y. Jung, N. Snook, and G. Zhang, 2019: Ensemble Kalman Filter assimilation of polarimetric radar observations for the 20 May 2013 Oklahoma tornadic supercell case. *Mon. Wea. Rev.*, **147**, 2511–2533, https://doi.org/10.1175/MWR-D-18-0251.1.

Rabin, R. M., and R. J. Doviak, 1989: Meteorological and astronomical influences on radar reflectivity in the convective boundary layer. *J. Appl. Meteor.*, **28**, 1226–1235, https://doi.org/10.1175/1520-0450(1989)028<1226:MAAIOR>2.0.CO;2.

Ryzhkov, A. V., and D. S. Zrnić, 2019: *Radar Polarimetry for Weather Observations.* Springer, 486 pp.

——, M. Pinksy, A. Pokrovsky, and A. Khain, 2011: Polarimetric radar observation operator for a cloud model with spectral microphysics. *J. Appl. Meteor. Climatol.*, **50**, 873–894, https://doi.org/10.1175/2010JAMC2363.1.

——, P. Zhang, H. Reeves, M. Kumjian, T. Tschallener, S. Troemel, and C. Simmer, 2016: Quasi-vertical profiles – A new way to look at polarimetric radar data. *J. Appl. Meteor. Climatol.*, **33**, 551–562, https://doi.org/10.1175/JTECH-D-15-0020.1.

Salazar, J. L., and Coauthors, 2019: An ultra-fast scan C-band Polarimetric Atmospheric Imaging Radar (PAIR). *2019 IEEE Int. Symp. on Phased Array Systems and Technology*, Waltham, MA, IEEE, 1–5, https://doi.org/10.1109/PAST43306.2019.9021042.

Schneider, D., and S. Sharp, 2007: Radar signatures of tropical cyclone tornadoes in Central North Carolina. *Wea. Forecasting*, **22**, 278–286, https://doi.org/10.1175/WAF992.1.

Schrom, R. S., and M. R. Kumjian, 2019: A probabilistic radar forward model for branched planar ice crystals. *J. Appl. Meteor. Climatol.*, **58**, 1245–1265, https://doi.org/10.1175/JAMC-D-18-0204.1.

——, ——, and Y. Lu, 2015: Polarimetric radar signatures of dendritic growth zones within Colorado winter storms. *J. Appl. Meteor. Climatol.*, **54**, 2365–2388, https://doi.org/10.1175/JAMC-D-15-0004.1.

——, M. van Lier-Walqui, M. R. Kumjian, J. Y. Harrington, A. A. Jensen, and Y.-S. Chen, 2021: Radar-based Bayesian estimation of ice crystal growth parameters within a microphysical model. *J. Atmos. Sci.*, **78**, 549–569, https://doi.org/10.1175/JAS-D-20-0134.1.

Schultz, L. A., and D. J. Cecil, 2009: Tropical cyclone tornadoes, 1950–2007. *Mon. Wea. Rev.*, **137**, 3471–3484, https://doi.org/10.1175/2009MWR2896.1.

Skinner, P. S., L. J. Wicker, P. L. Heinselman, and D. J. Stensrud, 2014: Initial analysis and forecasts of the 31 May 2013 El Reno tornadic storm: Impact from rapid-scan Phased Array Radar (PAR). *Special Symp. on Severe Local Storms: The Current State of the Science and Understanding Impacts*, Atlanta, GA, Amer. Meteor. Soc., 853, https://ams.confex.com/ams/94Annual/webprogram/Paper240997.html.

Snyder, J. C., H. B. Bluestein, Z. B. Wienhoff, C. M. Kuster, and D. W. Reif, 2020: An analysis of an ostensible anticyclonic tornado from 9 May 2016 using high-resolution, rapid-scan radar data. *Wea. Forecasting*, **35**, 1685–1712, https://doi.org/10.1175/WAF-D-20-0055.1.

Stein, T. H., R. J. Hogan, P. A. Clark, C. E. Halliwell, K. E. Hanley, H. W. Lean, J. C. Nicol, and R. S. Plant, 2015: The DYMECS project: A statistical approach for the evaluation of convective storms in high-resolution NWP models. *Bull. Amer. Meteor. Soc.*, **96**, 939–951, https://doi.org/10.1175/BAMS-D-13-00279.1.

Stensrud, D. J., and Coauthors, 2013: Progress and challenges with warn-on-forecast. *Atmos. Res.*, **123**, 2–16, https://doi.org/10.1016/j.atmosres.2012.04.004.

Stephens, G., D. Winker, J. Pelon, C. Trepte, D. Vane, C. Yuhas, T. L'Ecuyer, and M. Lebsock, 2018: CloudSat and CALIPSO within the A-Train: Ten years of actively observing the Earth system. *Bull. Amer. Meteor. Soc.*, **99**, 569–581, https://doi.org/10.1175/BAMS-D-16-0324.1.

Stratman, D. R., N. Yussouf, Y. Jung, T. A. Supinie, M. Xue, P. S. Skinner, and B. J. Putnam, 2020: Optimal temporal frequency of NSSL phased array radar observations for an experimental warn-on-forecast system. *Wea. Forecasting*, **35**, 193–214, https://doi.org/10.1175/WAF-D-19-0165.1.

Supinie, T. A., N. Yussouf, Y. Jung, M. Xue, J. Cheng, and S. Wang, 2017: Comparison of the analyses and forecasts of a tornadic supercell storm from assimilating phased-array radar and WSR-88D observations. *Wea. Forecasting*, **32**, 1379–1401, https://doi.org/10.1175/WAF-D-16-0159.1.

Tanamachi, R. L., and P. L. Heinselman, 2016: Rapid-scan, polarimetric observations of central Oklahoma severe storms on 31 May 2013. *Wea. Forecasting*, **31**, 19–42, https://doi.org/10.1175/WAF-D-15-0111.1.

——, ——, and L. J. Wicker, 2015: Impacts of a storm merger on the 24 May 2011 El Reno, Oklahoma tornadic supercell. *Wea. Forecasting*, **30**, 501–524, https://doi.org/10.1175/WAF-D-14-00164.1.

Thompson, T. E., and L. J. Wicker, 2009: Assimilation of phased array radar data for the analysis of the 29 May 2004 Oklahoma City supercell. University of Oklahoma, 92 pp.

Tobin, D. M., and M. R. Kumjian, 2017: Polarimetric radar and surface-based precipitation-type observations of ice pellet to freezing rain transitions. *Wea. Forecasting*, **32**, 2065–2082, https://doi.org/10.1175/WAF-D-17-0054.1.

Torres, S. M., and D. Schvartzman, 2020: A simulation framework to support the design and evaluation of adaptive scanning for phased-array weather radars. *J. Atmos. Oceanic Technol*., **37**, 2321–2339, https://doi.org/10.1175/JTECH-D-20-0087.1.

Tuftedal, K. S., M. M. French, and D. M. Kingfield, 2021: Observed bulk hook echo drop size distribution evolution in supercell tornadogenesis and tornadogenesis failure. *Mon. Wea. Rev.*, **149**, 2539–2557, https://doi.org/10.1175/MWR-D-20-0353.1.

Tulu, Z. C., S. J. Frasier, R. Janaswamy, and D. J. McLaughlin, 2006: Considerations for bistatic probing of clear-air winds in the atmospheric boundary layer. *Radio Sci.*, **41**, RS3003, https://doi.org/10.1029/2005RS003293.

Turner, D. D., and R. G. Ellingson, Eds., 2017: *The Atmospheric Radiation Measurement (ARM) Program: The First 20 Years*. *Meteor. Monogr.*, No. 57, Amer. Meteor. Soc., https://doi.org/10.1175/AMSMONOGRAPHS-D-15-0001.1.

van Leeuwen, P. J., 2009: Particle filtering in geophysical systems. *Mon. Wea. Rev.*, **137**, 4089–4114, https://doi.org/10.1175/2009MWR2835.1.

van Lier-Walqui, M., and Coauthors, 2016: On polarimetric radar signatures of deep convection for model evaluation: Columns of specific differential phase observed during MC3E. *Mon. Wea. Rev.*, **144**, 737–758, https://doi.org/10.1175/MWR-D-15-0100.1.

Varble, A., 2018: Erroneous attribution of deep convective invigoration to aerosol concentration. *J. Atmos. Sci.*, **75**, 1351–1368, https://doi.org/10.1175/JAS-D-17-0217.1.

Vivekanandan, J., L. Perez-Clifford, E. Loew, and A. Karboski, 2020: Airborne polarimetric Doppler phased array weather radar: Performance requirements and design specifications. *2020 IEEE Radar Conf. (RadarConf20)*, Florence, Italy, IEEE, 1–6, https://doi.org/10.1109/RadarConf2043947.2020.9266530.

Wakimoto, R. M., P. Stauffer, K. M. Butler, H. B. Bluestein, K. Thiem, J. Snyder, and J. Houser, 2015: Photogrammetric analysis of the 2013 El Reno tornado combined with mobile X-band polarimetric radar data. *Mon. Wea. Rev.*, **143**, 2657–2683, https://doi.org/10.1175/MWR-D-15-0034.1.

——, and Coauthors, 2016: Aerial damage survey of the 2013 El Reno tornado combined with mobile radar data. *Mon. Wea. Rev.*, **144**, 1749–1776, https://doi.org/10.1175/MWR-D-15-0367.1.

——, Z. Wienhoff, H. B. Bluestein, and D. Reif, 2018: The Dodge City tornadoes on 24 May 2016: Damage survey, photogrammetric analysis combined with mobile polarimetric radar data. *Mon. Wea. Rev.*, **146**, 3735–3771, https://doi.org/10.1175/MWR-D-18-0125.1.

——, ——, ——, D. J. Bodine, and J. M. Kurdzo, 2020: Mobile radar observations of the evolving debris field compared with a damage survey of the Shawnee, Oklahoma, tornado of 19 May 2013. *Mon. Wea. Rev.*, **148**, 1779–1803, https://doi.org/10.1175/MWR-D-19-0215.1.

Wang, D., S. E. Giangrande, Z. Feng, J. C. Hardin, and A. F. Prein, 2020: Updraft and downdraft core size and intensity as revealed by radar wind profilers: MCS observations and idealized model comparisons. *J. Geophys. Res. Atmos.*, **125**, e2019JD031774, https://doi.org/10.1029/2019JD031774.

Wang, X., H. G. Chipilski, C. H. Bishop, E. Satterfield, N. Baker, and J. Whittaker, 2021: A multiscale local gain form ensemble transform Kalman filter (MLGETKF). *Mon. Wea. Rev.*, **149**, 605–622, https://doi.org/10.1175/MWR-D-20-0290.1.

Weadon, M., P. Heinselman, D. Forsyth, J. Kimpel, W. E. Benner, and G. S. Torok, 2009: Multifunction phased array radar. *Bull. Amer. Meteor. Soc.*, **90**, 385–389, https://doi.org/10.1175/2008BAMS2666.1.

Weber, M., and Coauthors, 2021: Towards the next generation operational meteorological radar. *Bull. Amer. Meteor. Soc.*, **102**, E1357–E1383, https://doi.org/10.1175/BAMS-D-20-0067.1.

Wicker, L. J., T. E. Thompson, C. K. Potvin, and E. R. Mansell, 2012: Comparisons between analysis and prediction of convection using conventional and rapid-scan weather Doppler radar data. *26th Conf. on Severe Local Storms*, Nashville, TN, Amer. Meteor. Soc., 7.3, https://ams.confex.com/ams/26SLS/webprogram/Paper212018.html.

Wienhoff, Z. B., H. B. Bluestein, L. J. Wicker, J. C. Snyder, A. Shapiro, C. K. Potvin, J. B. Houser, and D. W. Reif, 2018: Applications of a spatially variable advection correction technique for temporal correction of dual-Doppler analyses of tornadic supercells. *Mon. Wea. Rev.*, **146**, 2949–2971, https://doi.org/10.1175/MWR-D-17-0360.1.

——, ——, D. W. Reif, R. M. Wakimoto, L. J. Wicker, and J. M. Kurdzo, 2020: Analysis of debris signature characteristics and evolution in the 24 May 2016 Dodge City, Kansas, tornadoes. *Mon. Wea. Rev.*, **148**, 5063–5086, https://doi.org/10.1175/MWR-D-20-0162.1.

Williams, C. R., 2012: Vertical air motion retrieved from dual-frequency profiler observations. *J. Atmos. Oceanic Technol.*, **29**, 1471–1480, https://doi.org/10.1175/JTECH-D-11-00176.1.

Wu, D., and Coauthors, 2018: The kinematics and microphysics of convection in the outer rainband of Typhoon Nida (2016) revealed by polarimetric radar. *Mon. Wea. Rev.*, **146**, 2147–2159, https://doi.org/10.1175/MWR-D-17-0320.1.

——, F. Zhang, X. Chen, A. Ryzhkov, K. Zhao, M. R. Kumjian, X. Chen, and P.-W. Chan, 2021: Evaluation of microphysics schemes in tropical cyclones using polarimetric radar observations: Convective precipitation in outer rainband. *Mon. Wea. Rev.*, **149**, 1055–1068, https://doi.org/10.1175/MWR-D-19-0378.1.

Wurman, J., and K. Kosiba, 2013: Finescale radar observations of tornado and mesoscale structures. *Wea. Forecasting*, **28**, 1157–1174, https://doi.org/10.1175/WAF-D-12-00127.1.

——, ——, T. White, and P. Robinson, 2021: Supercell tornadoes are much stronger and wider than damage-based rating indicate. *Proc. Natl. Acad. Sci. USA*, **118**, e2021535118, https://doi.org/10.1073/pnas.2021535118.

Xu, M., and T. Gal-Chen, 1993: A study of the convective boundary-layer dynamics using single Doppler radar measurements. *J. Atmos. Sci.*, **50**, 3641–3662, https://doi.org/10.1175/1520-0469(1993)050<3641:ASOTCB>2.0.CO;2.

Yarbus, A. L., 1967: *Eye Movements and Vision.* Plenum Press, 222 pp.

Yussouf, N., and D. J. Stensrud, 2010: Impact of phased-array radar observations over a short assimilation period: Observing system simulation experiments using an ensemble Kalman filter. *Mon. Wea. Rev.*, **138**, 517–538, https://doi.org/10.1175/2009MWR2925.1.

Zhang, J., L. Tang, S. Cocks, P. Zhang, A. Ryzhkov, K. Howard, C. Langston, and B. Kaney, 2020: A dual-polarization radar synthetic QPE for operations. *J. Hydrometeor.*, **21**, 2507–2521, https://doi.org/10.1175/JHM-D-19-0194.1.

Zrnić, D. S., and A. V. Ryzhkov, 1999: Polarimetry for weather surveillance radars. *Bull. Amer. Meteor. Soc.*, **80**, 389–406, https://doi.org/10.1175/1520-0477(1999)080<0389:PFWSR>2.0.CO;2.